

# The “Indenyl Effect” in Zirconocene Dihydride Chemistry

Christopher A. Bradley, Ivan Keresztes, Emil Lobkovsky, and Paul J. Chirik\*

Department of Chemistry and Chemical Biology, Baker Laboratory, Cornell University,  
Ithaca, New York 14853

Received January 11, 2006

The second-order rate constants for the insertion of cyclohexene into substituted bis(indenyl)zirconocene dihydrides,  $(\eta^5\text{-C}_9\text{H}_5\text{-1,3-R}_2)_2\text{ZrH}_2$  ( $\text{R} = \text{SiMe}_3, \text{CHMe}_2$ ), to yield the cyclohexyl hydride complexes have been measured. Comparison of these values to the corresponding tetrahydroindenyl derivatives  $(\eta^5\text{-C}_9\text{H}_9\text{-1,3-R}_2)_2\text{ZrH}_2$  reveals significantly faster insertion reactions for the bis(indenyl) compounds. Accordingly, primarily  $\sigma$ -donating ligands such as  $\text{PMe}_3$ ,  $\text{PET}_3$ , and tetrahydrothiophene coordinate to  $(\eta^5\text{-C}_9\text{H}_5\text{-1,3-(CHMe}_2)_2)_2\text{ZrH}_2$  to form  $(\eta^5\text{-C}_9\text{H}_5\text{-1,3-(CHMe}_2)_2)_2\text{ZrH}_2(\text{L})$  compounds, one of which ( $\text{L} = \text{PMe}_3$ ) has been structurally characterized. In contrast, the more electron-rich zirconocene tetrahydroindenyl dihydrides exhibit weaker binding in solution. Taken together, these results establish an “indenyl effect” in zirconocene hydride chemistry likely arising from increased electrophilicity of the metal center, rather than a change in hapticity along the reaction coordinate.

## Introduction

Bis(indenyl)- and related bis(tetrahydroindenyl)zirconium(IV) dihalide and dialkyl complexes, when treated with the appropriate activator, constitute some of the most active and selective catalysts known for ethylene and  $\alpha$ -olefin polymerization.<sup>1</sup> Despite intense interest from both academic and industrial laboratories, little is known about the “indenyl effect”, replacing indenyl ligands with cyclopentadienyl or tetrahydroindenyl rings, as it pertains to fundamental transformations relevant to olefin polymerization.<sup>2</sup> Classically, the “indenyl effect” refers to the enhanced rates of associative substitution observed upon replacement of cyclopentadienyl rings with indenyl ligands<sup>3</sup> and has since been generalized to include increased catalytic activity with the latter ligand class.<sup>4</sup> The origin of this effect has traditionally been attributed to the ability of the indenyl ring to undergo “slippage” from  $\eta^5$  to  $\eta^3$  hapticity. This haptotropic flexibility is facilitated by the gain in aromaticity of the benzo ring and serves to open a coordination site to accommodate the incoming nucleophile. Recently, this classical description has been reevaluated in terms of a ground-state effect, rationalized by distinct  $\eta^3$ : $\eta^2$ -indenyl bonding, where two of the five metal–carbon bonds are longer than the other three.<sup>5</sup>

With respect to metallocene-catalyzed olefin polymerization, Collins and co-workers have compared the activity and stereoselectivity of indenyl- and tetrahydroindenyl-ligated zirconocene

catalysts in polypropylene synthesis.<sup>6</sup> When activated with an excess of methylalumoxane (MAO), *rac*-(EBI)ZrCl<sub>2</sub> (EBI = ethylenebis(indenyl)) produced faster rates of monomer consumption and higher polymer yields as compared to the tetrahydroindenyl derivative *rac*-(EBTHI)ZrCl<sub>2</sub> (EBTHI = ethylenebis(tetrahydroindenyl)). Caution needs to be exercised when interpreting these data, as the observed differences are likely a composite of several processes, each potentially with a different “indenyl effect”. Because the propagating species is now generally accepted as a coordinatively (or doubly) unsaturated zirconocenium alkyl cation,<sup>1,7</sup> indenyl ring slippage to accommodate the incoming olefin may seem unlikely.<sup>8</sup> However, Jordan and co-workers have reported the synthesis of an *ansa*-hafnocene diamide complex,  $[\text{Me}_2\text{Si}(\eta^5\text{-1-C}_9\text{H}_6)(\eta^3\text{-2-C}_9\text{H}_6)]\text{Hf}(\text{NMe}_2)_2$ , that adopts a “slipped” indenyl ring in the ground state.<sup>9</sup> Although this compound is not a propagating species in olefin polymerization, it does demonstrate that ring slippage can occur, at least in the ground state, of formally unsaturated complexes.

To determine if there are differences, e.g. an “indenyl effect”, on fundamental transformations relevant to olefin polymerization and other catalytic reactions involving group 4 metallocenes,<sup>10</sup> we initiated a study directly comparing rates of olefin insertion and the thermodynamic preferences for ligand coordination with bis(indenyl) and the corresponding bis(tetrahydroindenyl)-

(1) (a) Brintzinger, H. H.; Fischer, D.; Mülhaupt, R.; Rieger, B.; Waymouth, R. M. *Angew. Chem., Int. Ed. Engl.* **1995**, *34*, 1143. (b) Alt, H. G.; Köppl, A. *Chem. Rev.* **2000**, *100*, 1205. (c) Coates, G. W. *Chem. Rev.* **2000**, *100*, 1223. (d) Resconi, L.; Cavallo, L.; Fait, A.; Piemontesi, F. *Chem. Rev.* **2000**, *100*, 1253.

(2) For recent mechanistic studies with zirconocene olefin polymerization catalysts see: (a) Yang, P.; Baird, M. *Organometallics* **2005**, *24*, 6005. (b) Yang, P.; Baird, M. *Organometallics* **2005**, *24*, 6013. (c) Chirik, P. J.; Dalleska, N. F.; Henling, L. M.; Bercaw, J. E. *Organometallics* **2005**, *24*, 2789. (d) Bochmann, M. *J. Organomet. Chem.* **2004**, *689*, 3982. (e) Sillars, D. R.; Landis, C. R. *J. Am. Chem. Soc.* **2003**, *125*, 9894.

(3) (a) Rerek, M. E.; Basolo, F. *J. Am. Chem. Soc.* **1984**, *106*, 5908. (b) Kakkar, A. K.; Taylor, N. J.; Marder, T. J.; Shen, N.; Hallinan, N.; Basolo, F. *Inorg. Chim. Acta* **1992**, *198–200*, 219. (c) Wescott, S. A.; Kakkar, A. K.; Stringer, G.; Taylor, N. J.; Marder, T. B. *J. Organomet. Chem.* **1990**, *394*, 777. (d) O'Connor, J. M.; Casey, C. P. *Chem. Rev.* **1987**, *87*, 307.

(4) Trost, B. M.; Toste, F. D.; Pinkerton, A. B. *Chem. Rev.* **2001**, *101*, 2067.

(5) (a) Calhorda, M. J.; Romão, C. C.; Veiros, L. F. *Chem. Eur. J.* **2002**, *8*, 868. (b) Zargarian, D. *Coord. Chem. Rev.* **2002**, *233–234*, 157. (c) Trnka, T. M.; Bonanno, J. B.; Bridgewater, B. M.; Parkin, G. *Organometallics* **2001**, *20*, 3255. (d) Calhorda, M. J.; Veiros, L. F. *Coord. Chem. Rev.* **1999**, *185–186*, 37.

(6) Collins, S.; Gautler, W. J.; Holden, D. A.; Kuntz, B. A.; Taylor, N. J.; Ward, D. G. *Organometallics* **1991**, *10*, 2061.

(7) Rappe, A. K.; Skiff, W. M.; Casewit, C. J. *Chem. Rev.* **2000**, *100*, 1435.

(8) An *ansa*-titanocene imido complex with a “slipped” indenyl ligand that serves as an initiator for methyl methacrylate polymerization has been reported: Jin, J.; Chen, Y.-X. *Organometallics* **2002**, *21*, 13.

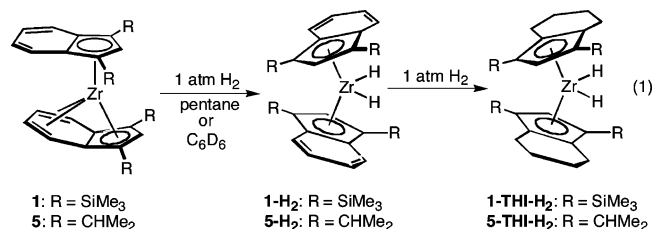
(9) Christopher, J. N.; Jordan, R. F.; Petersen, J. F.; Young, V. G. *Organometallics* **1997**, *16*, 3044.

(10) (a) Troutman, M. V.; Appella, D. H.; Buchwald, S. L. *J. Am. Chem. Soc.* **1999**, *121*, 4916. (b) Gribkov, D. V.; Hultsch, K. C. *Angew. Chem., Int. Ed.* **2004**, *43*, 5542. (c) Cesati, R. R.; de Armas, J.; Hoveyda, A. H. *Org. Lett.* **2002**, *4*, 395. (d) Michael, F. E.; Duncan, A. P.; Sweeney, Z. K.; Bergman, R. G. *J. Am. Chem. Soc.* **2005**, *127*, 1752.

zirconium dihydride complexes. In the past, such a study has been limited because bis(indenyl)zirconium dihydrides have not been synthetically accessible. Having recently prepared these compounds,<sup>16</sup> herein we report that the “indenyl effect” is primarily a consequence of more electrophilic metal centers engendered by an electron-withdrawing ligand rather than a dramatic change in hapticity along the reaction coordinate.

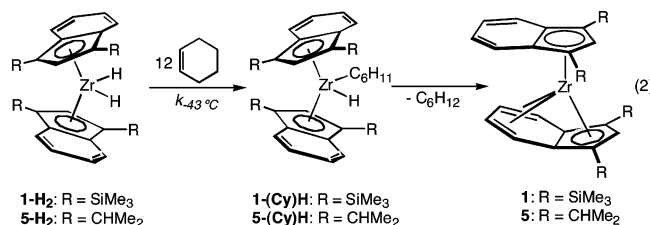
## Results and Discussion

**Kinetics of Olefin Insertion.** Recently, our laboratory has described the synthesis<sup>11,12</sup> of a family of unusual ( $\eta^9$ -indenyl)-( $\eta^5$ -indenyl)zirconium sandwich compounds. Interestingly, characterization in both solution and the solid state<sup>12</sup> established that all nine carbons of one indenyl ring are bound to the zirconium, providing the first examples of mononuclear  $\eta^9$  coordination.<sup>13</sup> These compounds highlight the ability of the indenyl ligand to smoothly change hapticity to meet the electronic demands of the metal center and serve as convenient starting materials for a host of interesting bent bis(indenyl)-zirconium derivatives.<sup>14</sup> As part of our ongoing studies exploring the reactivity of these compounds, we have discovered that treatment of ( $\eta^9$ -C<sub>9</sub>H<sub>5</sub>-1,3-R<sub>2</sub>)( $\eta^5$ -C<sub>9</sub>H<sub>5</sub>-1,3-R<sub>2</sub>)Zr (R = SiMe<sub>3</sub> (**1**), CHMe<sub>2</sub> (**5**)) with H<sub>2</sub> resulted in oxidative addition to furnish the derivatives ( $\eta^5$ -C<sub>9</sub>H<sub>5</sub>-1,3-R<sub>2</sub>)<sub>2</sub>ZrH<sub>2</sub> (R = SiMe<sub>3</sub> (**1-H<sub>2</sub>**), CHMe<sub>2</sub> (**5-H<sub>2</sub>**))<sup>15</sup> with the benzo rings intact and  $\eta^5$  coordination restored (eq 1).<sup>16</sup> Continued H<sub>2</sub> addition at 23 °C resulted in



hydrogenation of the six-membered rings and yielded the corresponding bis(tetrahydroindenyl)zirconocene dihydrides ( $\eta^5$ -C<sub>9</sub>H<sub>9</sub>-1,3-R<sub>2</sub>)<sub>2</sub>ZrH<sub>2</sub> (R = SiMe<sub>3</sub> (**1-THI-H<sub>2</sub>**), CHMe<sub>2</sub> (**5-THI-H<sub>2</sub>**)) (eq 1). It should be noted that ring hydrogenation is relatively slow at ambient temperature and the preparation of the tetrahydroindenyl derivatives is best carried out at 60 °C.

With both bis(indenyl)zirconocene and the corresponding bis(tetrahydroindenyl)zirconocene dihydrides in hand, the “indenyl effect” on the rate of olefin insertion was evaluated. Addition of an excess (12 equiv) of cyclohexene to **1-H<sub>2</sub>** and **5-H<sub>2</sub>** resulted in clean and quantitative conversion to ( $\eta^5$ -C<sub>9</sub>H<sub>5</sub>-1,3-R<sub>2</sub>)<sub>2</sub>Zr(C<sub>6</sub>H<sub>11</sub>)H (R = SiMe<sub>3</sub> (**1-(Cy)H**), CHMe<sub>2</sub> (**5-(Cy)H**)) (eq 2). At 23 °C, the silylated bis(indenyl)zirconocene cyclohexyl hydride **1-(Cy)H** underwent rapid reductive elimination of alkane, regenerating the sandwich complex **1**. A similar cyclohexane reductive elimination process occurred with **5-(Cy)H**, although longer reaction times, on the order of 1 h, were required for complete conversion. Both sandwich complexes were

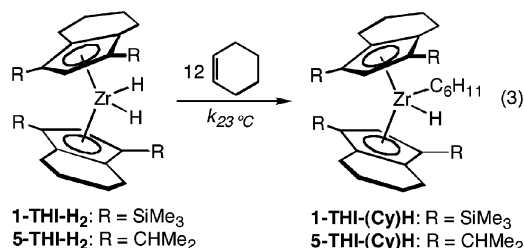


unreactive toward excess cyclohexene, as judged by <sup>1</sup>H NMR spectroscopy.

To avoid complications arising from competitive cyclohexane reductive elimination, rate constants for olefin insertion were determined by <sup>1</sup>H NMR spectroscopy at -43 °C with 0.020 M solutions of zirconocene dihydride under pseudo-first-order conditions with 12 equiv (0.253 M) of olefin. Using this procedure, second-order rate constants of 1.2(2) × 10<sup>-2</sup> and 5.5(2) × 10<sup>-3</sup> M<sup>-1</sup> s<sup>-1</sup> (Table 1) were measured for **1-H<sub>2</sub>** and **5-H<sub>2</sub>**, respectively. Previous studies on isobutene insertion with highly substituted bis(cyclopentadienyl)zirconocene dihydrides have demonstrated a profound steric effect, where slight reduction in the size of the ring substituents dramatically increased the rate of olefin insertion.<sup>17</sup> For example, the rate constant for ( $\eta^5$ -C<sub>5</sub>Me<sub>5</sub>)( $\eta^5$ -C<sub>5</sub>Me<sub>4</sub>H)ZrH<sub>2</sub> insertion was approximately 3800 times that for ( $\eta^5$ -C<sub>5</sub>Me<sub>5</sub>)<sub>2</sub>ZrH<sub>2</sub>.<sup>17</sup>

For the bis(indenyl)zirconocene dihydrides **1-H<sub>2</sub>** and **5-H<sub>2</sub>**, the compound bearing the tertiary silyl substituents undergoes cyclohexene insertion slightly faster than the isopropyl-substituted compound. The increase in second-order rate constant is most likely a result of the relative electrophilicities of the two zirconocene dihydrides. Previous work from our laboratory<sup>18,19</sup> and others<sup>20</sup> has demonstrated that silyl-substituted indenyl and cyclopentadienyl ligands engender more electrophilic metal centers than their alkylated counterparts.

Similar kinetic studies were also performed with the substituted bis(tetrahydroindenyl)zirconium dihydrides **1-THI-H<sub>2</sub>** and **5-THI-H<sub>2</sub>**. Under pseudo-first-order conditions with 12 equiv of cyclohexene, both **1-THI-H<sub>2</sub>** and **5-THI-H<sub>2</sub>** participated in olefin insertion to yield the cyclohexyl hydride compounds ( $\eta^5$ -C<sub>9</sub>H<sub>9</sub>-1,3-R<sub>2</sub>)<sub>2</sub>Zr(C<sub>6</sub>H<sub>11</sub>)H (R = SiMe<sub>3</sub> (**1-THI-(Cy)H**), CHMe<sub>2</sub> (**5-THI-(Cy)H**)) (eq 3). Second-order rate constants were



determined at 23 °C, as the reaction rates were too slow to be conveniently measured at -43 °C. As with the indenyl-substituted derivatives, the silylated zirconocene dihydride **1-THI-H<sub>2</sub>** inserts cyclohexene slightly faster than the alkyl-substituted compound **5-THI-H<sub>2</sub>**. Significantly, both tetrahydroindenyl compounds react much more slowly with olefin than do the indenyl complexes. While direct comparisons cannot be

(11) Bradley, C. A.; Lobkovsky, E.; Chirik, P. J. *J. Am. Chem. Soc.* **2003**, *125*, 8110.

(12) Bradley, C. A.; Keresztes, I.; Lobkovsky, E.; Young, V. G.; Chirik, P. J. *J. Am. Chem. Soc.* **2004**, *126*, 16937.

(13) Veiros, L. F. *Chem. Eur. J.* **2005**, *11*, 2505.

(14) Bradley, C. A.; Lobkovsky, E.; Keresztes, I.; Chirik, P. J. *J. Am. Chem. Soc.* **2005**, *127*, 10291.

(15) The numbering scheme is taken from that initially described in ref 18.

(16) Bradley, C. A.; Keresztes, I.; Lobkovsky, E.; Chirik, P. J. Submitted for publication.

(17) Chirik, P. J.; Bercaw, J. E. *Organometallics* **2005**, *24*, 5407.

(18) Bradley, C. A.; Flores-Torres, S.; Lobkovsky, E.; Abruña, H. D.; Chirik, P. J. *Organometallics* **2004**, *23*, 5332.

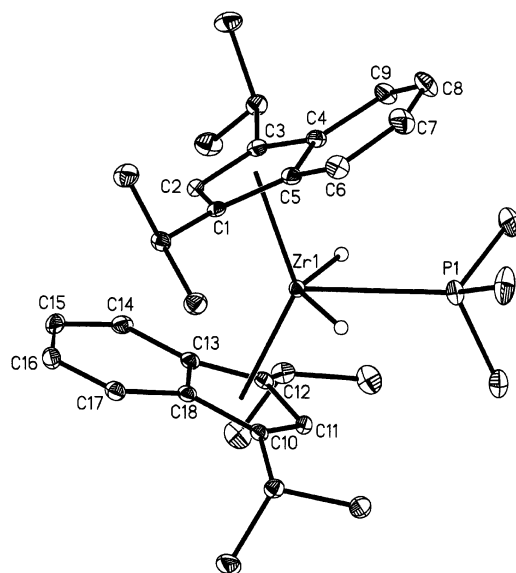
(19) Pool, J. A.; Lobkovsky, E.; Chirik, P. J. *J. Am. Chem. Soc.* **2003**, *125*, 2241.

(20) Zachmanoglou, C. E.; Docrat, A.; Bridgewater, B. M.; Parkin, G. E.; Brandow, C. G.; Bercaw, J. E.; Jardine, C. N.; Lyall, M.; Green, J. C.; Keister, J. B. *J. Am. Chem. Soc.* **2002**, *124*, 9525.

**Table 1.** Rate Constants for Cyclohexene Insertion with Bis(indenyl)- and Bis(tetrahydroindenyl)zirconium Dihydrides

compound	$k_{\text{ins}}$ ( $\text{M}^{-1} \text{s}^{-1}$ )
<b>1-H<sub>2</sub></b> <sup>a</sup>	$1.2(2) \times 10^{-2}$
<b>5-H<sub>2</sub></b> <sup>a</sup>	$5.5(2) \times 10^{-3}$
<b>1-THI-H<sub>2</sub></b> <sup>b</sup>	$3.4(6) \times 10^{-4}$
<b>5-THI-H<sub>2</sub></b> <sup>b</sup>	$3.0(4) \times 10^{-5}$

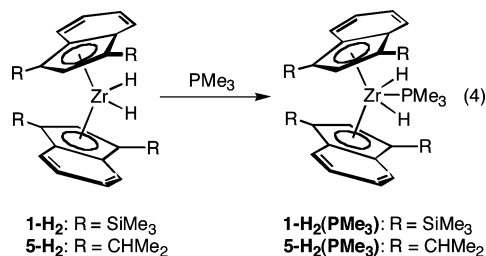
<sup>a</sup> Determined at  $-43$  °C. <sup>b</sup> Determined at  $23$  °C.

**Figure 1.** Molecular structure of **5-H<sub>2</sub>(PMe<sub>3</sub>)** with 30% probability ellipsoids. Hydrogen atoms, except for the zirconium hydrides, are omitted for clarity.

made due to our inability to determine rate constants at the same temperature assuming typical activation parameters observed for a second-order insertion reaction,<sup>17</sup> the indenyl complexes are approximately 2000–12,000 times more reactive than their saturated counterparts.

**Coordination of Principally  $\sigma$ -Donating Ligands.** One possibility for the observed differences in the second-order rate constants for cyclohexene insertion is a classic “indenyl effect” due to a change in hapticity from  $\eta^5$  to  $\eta^3$  along the reaction coordinate. To experimentally test this hypothesis, the dihydride complexes were treated with a series of  $\sigma$ -donors to determine if a “slipped” bis(indenyl)zirconium dihydride ligand adduct could be observed or even isolated.

Addition of  $\text{PMe}_3$  to a pentane solution of **1-H<sub>2</sub>** or **5-H<sub>2</sub>** immediately generated the corresponding phosphine adducts ( $\eta^5$ -C<sub>9</sub>H<sub>5</sub>-1,3-R<sub>2</sub>)<sub>2</sub>ZrH<sub>2</sub>(PMe<sub>3</sub>) (R = SiMe<sub>3</sub>, (**1-H<sub>2</sub>(PMe<sub>3</sub>)**), R = CHMe<sub>2</sub> (**5-H<sub>2</sub>(PMe<sub>3</sub>)**)) (eq 4). Both complexes have been



characterized by multinuclear NMR spectroscopy and, in the case of **5-H<sub>2</sub>(PMe<sub>3</sub>)**, single-crystal X-ray diffraction. The solid-state structure of the compound is presented in Figure 1, and selected metrical parameters are reported in Table 2. For

**Table 2.** Selected Metrical Parameters for **5-H<sub>2</sub>(PMe<sub>3</sub>)** and **5-H<sub>2</sub>**

	<b>5-H<sub>2</sub>(PMe<sub>3</sub>)</b>	<b>5-H<sub>2</sub></b>
slip distortion, <sup>a</sup> Å	0.059(2)	0.066(1)
fold angle, <sup>b</sup> deg	0.163(2)	1.9(3)
rotational angle, <sup>c</sup> deg	163.2(3)	88.7(3)
$\alpha$ , deg	47.6(2)	33.2(3)
$\beta$ , deg	132.4(2)	146.8(3)
$\gamma$ , deg	136.3(2)	144.8(3)
$\tau$ , deg	2	-1
$\eta^3$ angle, <sup>d</sup> deg	9.5(3)	7.4(1)
hinge angle, <sup>e</sup> deg	12.2(1)	8.1(2)
H–Zr–H, deg	9.1(2)	129.0(9)
	129.0(9)	95.6(2)

<sup>a</sup> Average distance of the bridgehead metal-carbon bonds—average metal-carbon bond distance of the carbons unique to the five-membered ring. <sup>b</sup> Angle formed between the intersection of the planes defined by the four carbons proximal to the benzo ring and the three carbons unique to the five-membered ring. <sup>c</sup> Angle formed between the planes defined by Zr(1), C(2) and the centroid between C(4)–C(5) for each indenyl ligand. <sup>d</sup> Defined as the angle between the planes of the three carbons unique to the five-membered ring and four carbons unique to the six-membered ring. <sup>e</sup> Defined as the angle between the planes of the five carbons in the five-membered ring and the six carbons in the benzo ring.

comparison, the metrical parameters<sup>16</sup> of the dihydride complex **5-H<sub>2</sub>** are also presented. The indenyl rings in **5-H<sub>2</sub>(PMe<sub>3</sub>)** adopt a principally anti conformation with a rotational angle of  $163.2(3)^\circ$  (Table 2). This geometry is quite different from that of the gauche rotamer (rotational angle  $88.7(3)^\circ$ ) observed in the solid-state structure of the corresponding dihydride complex **5-H<sub>2</sub>**.

One other notable structural difference between the dihydride **5-H<sub>2</sub>** and the phosphine adduct **5-H<sub>2</sub>(PMe<sub>3</sub>)** is the slight deviation of one of the indenyl rings from  $\eta^5$  hapticity in the latter compound. While the structural parameters are far from what would be considered bona fide  $\eta^3$  hapticity,<sup>5,9,21</sup> a larger slip distortion of  $0.163(2)$  Å is observed as compared to the values of  $0.059(2)$  and  $0.066(1)$  Å found in the other indenyl ligand and in **5-H<sub>2</sub>**, respectively. By way of calibration, metallocenes with slip distortions less than  $0.30$  Å are classified as having  $\eta^5$  hapticity.<sup>22</sup> Both the “ $\eta^3$  angle”<sup>21a</sup> and the “hinge angle” also deviate from typical  $\eta^5$  bonding but are far from what is typically considered a true  $\eta^3$  structure.

The solid-state structure of **5-H<sub>2</sub>(PMe<sub>3</sub>)** also confirms coordination of the phosphine in the central position of the zirconocene wedge. The isomer where the neutral ligand is coordinated in the central position of the metallocene wedge is common in group 4 metallocene chemistry, and a similar *ansa*-bis(cyclopentadienyl)zirconocene dihydride  $\text{PMe}_3$  complex has

(21) (a) Merola, J. S.; Kacmarcik, E. T.; Van Engen, D. *J. Am. Chem. Soc.* **1986**, *108*, 329. (b) Kowaleski, R. M.; Rheingold, A. L.; Troglor, W. C.; Basolo, F. *J. Am. Chem. Soc.* **1986**, *108*, 2460. (c) Husebo, T. L.; Jensen, C. M. *Organometallics* **1995**, *14*, 1087. (d) Wescott, S. A.; Kakkur, A. K.; Taylor, N. J.; Roe, D. C.; Marder, T. B. *Can. J. Chem.* **1999**, *77*, 205. (e) Baker, R. T.; Tulip, T. H. *Organometallics* **1986**, *5*, 839.

(22) Faller, J. W.; Crabtree, R. H.; Habib, A. *Organometallics* **1985**, *4*, 929.



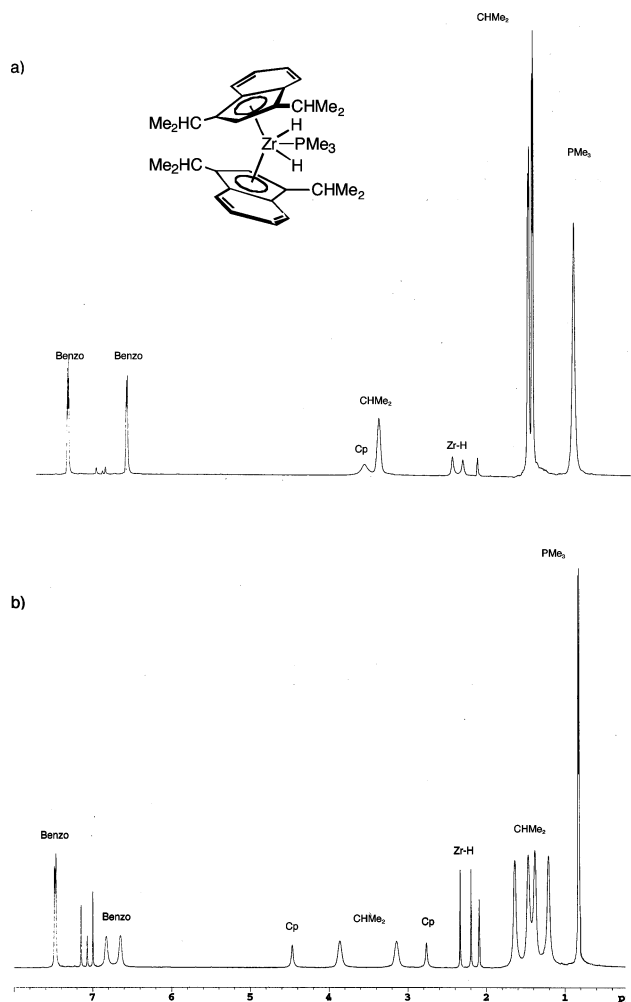


**Figure 2.**  $^1\text{H}$  NMR spectra of  $5\text{-H}_2(\text{PMe}_3)$  at (a)  $23\text{ }^\circ\text{C}$  and (b)  $-54\text{ }^\circ\text{C}$  in toluene- $d_8$ .

been crystallographically characterized.<sup>23</sup> The zirconium–phosphorus bond distance of  $2.7166(6)\text{ \AA}$  found in  $5\text{-H}_2(\text{PMe}_3)$  is in the range typically observed for phosphine complexes of zirconocenes.<sup>24</sup>

Because the kinetics of olefin insertion were measured in arene solvents and the hapticity of the indenyl ligands in the solid state may not reflect the actual coordination mode in solution, a series of NMR studies were conducted on  $5\text{-H}_2(\text{PMe}_3)$  and related compounds. At  $23\text{ }^\circ\text{C}$  in toluene- $d_8$ , the  $^1\text{H}$  NMR spectrum (Figure 2) of  $5\text{-H}_2(\text{PMe}_3)$  exhibits the number of resonances expected for a  $C_{2v}$ -symmetric zirconocene dihydride with a phosphine ligand occupying the central position of the metallocene wedge. Notably, the resonance for the cyclopentadienyl hydrogens, the isopropyl methines, and the zirconium hydrides are broadened, consistent with a dynamic process on the NMR time scale. Cooling the sample to  $-54\text{ }^\circ\text{C}$  resulted in decoalescence of the resonances and produced the number of peaks consistent with a  $C_s$ -symmetric compound with two inequivalent indenyl rings.

The inequivalence of the indenyl ligands could be a result of ring slippage, where one ring is  $\eta^5$  bound and the other is  $\eta^3$  coordinated,<sup>25</sup> restricted ring rotation on the NMR time scale, or a combination of both. Inspection of the crystallographic data

(23) Lee, H.; Desrosiers, P. J.; Guzei, I.; Rheingold, A. L.; Parkin, G. J. *Am. Chem. Soc.* **1998**, *120*, 3255.

(24) (a) Visser, C.; van den Hende, J. R.; Meetsma, A.; Hessen, B.; Teuben, J. H. *Organometallics* **2001**, *20*, 1620. (b) van den Hende, J. R.; Hessen, B.; Meetsma, A.; Teuben, J. H. *Organometallics* **1990**, *9*, 537.

**Table 3.**  $^{13}\text{C}$  NMR Shifts of Quaternary Indenyl Carbons Determined at  $-70\text{ }^\circ\text{C}$  in Toluene- $d_8$

compd	$^{13}\text{C}$ NMR $\delta$ (ppm)
$\text{Li}(\text{THF})_n[\text{C}_9\text{H}_7]^a$	120.64
$\text{Li}(\text{THF})_n[\text{C}_9\text{H}_5\text{-1,3-(SiMe}_3)_2]^b$	136.44
$\text{Li}(\text{THF})_n[\text{C}_9\text{H}_5\text{-1,3-(CHMe}_2)_2]^b$	129.33
<b>5-H<sub>2</sub>(PMe<sub>3</sub>)</b>	116.09
	120.34
<b>10-H<sub>2</sub>(PMe<sub>3</sub>)</b>	117.14
$[\text{Me}_2\text{Si}(\eta^5\text{-1-C}_9\text{H}_6)(\eta^3\text{-2-C}_9\text{H}_6)]\text{Hf}(\text{NMe}_2)_2^c$	133.8
	134.8

<sup>a</sup> Spectrum determined in the presence of 3.3 equiv of THF to maintain solubility. <sup>b</sup> Five equivalents of THF added. <sup>c</sup> Data taken from ref 9.

established chemically distinct rings in the solid state, differing both by their coordination to the zirconium center and by their relative orientations. One ring is partially “slipped” and has its benzo ring positioned over the metallocene wedge and hence the  $\text{PMe}_3$  ligand, while the ring adopting more traditional  $\eta^5$  hapticity has its benzo ring directed toward the narrow portion of the bent metallocene away from the wedge. Either of these phenomena could be the origin of the appearance of inequivalent ligands at low temperature by NMR spectroscopy.

Of these two possibilities, the experimental data are most consistent with restricted indenyl ring rotation as the origin of the dynamic process. Merola and others<sup>21</sup> have reported diagnostic NMR spectral changes for  $\eta^3$ -coordinated indenyl ligands. Specifically, the carbons at the ring junction shift substantially downfield in the  $^{13}\text{C}$  NMR spectrum upon ring slippage. It should be noted that most of these examples are based on late-transition metals, particularly rhodium and iridium. For early transition metals, Jordan has also noted similar spectral changes, albeit to a lesser extent, with the “slipped” hafnocene diamide complex  $[\text{Me}_2\text{Si}(\eta^5\text{-1-C}_9\text{H}_6)(\eta^3\text{-2-C}_9\text{H}_6)]\text{Hf}(\text{NMe}_2)_2$ .<sup>9</sup> Downfield-shifted ring junction carbons are reported at 133.8 and 134.8 ppm (Table 3) for the  $\eta^3$ -bound indenyl.

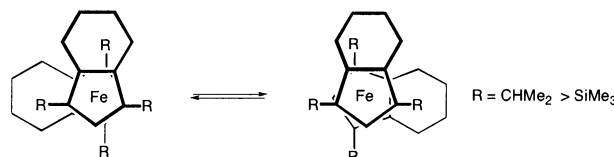
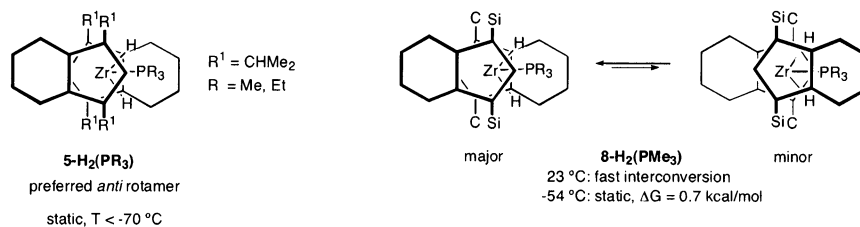
The toluene- $d_8$   $^{13}\text{C}$  NMR spectrum of  $5\text{-H}_2(\text{PMe}_3)$  at  $-70\text{ }^\circ\text{C}$  exhibits two distinct resonances for the ring junction carbons, consistent with a  $C_s$ -symmetric complex with inequivalent indenyl rings. These resonances appear at 116.09 and 120.34 ppm and were assigned with a two-dimensional g-HMBC experiment as described previously.<sup>9</sup> Significantly, the two peaks appear at similar chemical shifts with respect to each other, suggesting the same ( $\eta^5$ ) hapticity. Also contained in Table 3 are the  $^{13}\text{C}$  NMR shifts for the free indenide anions. Increasing the substitution on the indenyl ring results in a downfield shifting of the ring junction carbons and may be indicative of different degrees of aggregation and interaction with the lithium counterion.<sup>26</sup> On the basis of the correlation established by Köhler<sup>27</sup> and others,<sup>21d,e</sup> the relatively upfield shifts observed in the dihydride ligand adducts support  $\eta^5$  hapticity and hence restricted ring rotation as the origin of the dynamics rather than a shift to distinct  $\eta^3$  coordination.

At  $-54\text{ }^\circ\text{C}$ , the toluene- $d_8$   $^1\text{H}$  NMR spectrum of  $5\text{-H}_2(\text{PMe}_3)$  exhibits two upfield-shifted cyclopentadienyl hydrogens centered at 2.76 and 4.47 ppm. While slightly upfield shifted cyclopentadienyl resonances (5.64 versus 5.90 ppm) are observed for

(25) (a) Gonçalves, I. S.; Ribeiro-Claro, P.; Romão, C. C.; Royo, B.; Taveres, Z. M. *J. Organomet. Chem.* **2002**, *648*, 270. (b) Gonçalves, I. S.; Romão, C. C. *J. Organomet. Chem.* **1995**, *48*, 155.

(26) (a) Paquette, L. A.; Bauer, W.; Sivik, M. R.; Bühl, M.; Feigel, M.; Schleyer, P. v. R. *J. Am. Chem. Soc.* **1990**, *112*, 8776. (b) Jiao, H.; Schleyer, P. v. R.; Mo, Y.; McAllister, M. A.; Tidwell, T. T. *J. Am. Chem. Soc.* **1997**, *119*, 7075. (c) Paquette, L. A.; Sivik, M. R.; Bauer, W.; Schleyer, P. v. R. *Organometallics* **1994**, *13*, 4919. (d) Sivik, M. R.; Bauer, W.; Schleyer, P. v. R.; Paquette, L. A. *Organometallics* **1996**, *15*, 5202.

(27) Köhler, F. H. *Chem. Ber.* **1974**, *107*, 570.

**Bis(indenyl)iron Complexes: Gauche Conformers Preferred****Bis(indenyl)zirconium Phosphine Dihydrides: Anti Conformers Preferred**

**Figure 3.** Rotamers and conformational dynamics of bis(indenyl)iron and -zirconium dihydride ligand adducts.

$[\text{Me}_2\text{Si}(\eta^5\text{-1-C}_9\text{H}_6)(\eta^3\text{-2-C}_9\text{H}_6)]\text{Hf}(\text{NMe}_2)_2$ ,<sup>9</sup> the chemical shifts observed with **5-H<sub>2</sub>(PMe<sub>3</sub>)** are believed to be a result of transannular ring currents.<sup>14,21a</sup> In the anti ring conformation, both inequivalent cyclopentadienyl hydrogens are oriented over the benzo substituents of the opposite ring. Another notable feature of the static <sup>1</sup>H NMR spectrum of **5-H<sub>2</sub>(PMe<sub>3</sub>)** is the observation of a doublet ( $J = 68\text{ Hz}$ ) centered at 2.24 ppm, assigned as the equivalent zirconium hydrides. This peak does not change significantly with temperature, collapses to a singlet upon decoupling to <sup>31</sup>P, and disappears completely upon preparation of **5-D<sub>2</sub>(PMe<sub>3</sub>)**. Observation of a monomeric zirconocene hydride resonance this far upfield is consistent with a coordinatively saturated complex with a neutral ligand coordinated in the central position of the metallocene wedge.<sup>28</sup>

The solution structure of **5-H<sub>2</sub>(PMe<sub>3</sub>)** was further interrogated with a two-dimensional NOESY NMR experiment conducted in the static limit at  $-54\text{ }^\circ\text{C}$  in toluene-*d*<sub>8</sub> with a mixing time of 250 ms. The zirconium hydride has cross-peaks with the two isopropyl methyl groups centered at 1.39 and 1.47 ppm, as well as the benzo resonance at 7.47 ppm. Importantly, only one of the two inequivalent cyclopentadienyl hydrogens, that at 4.46 ppm, has a cross-peak with the zirconium hydride, establishing its orientation over the metallocene wedge. This cyclopentadienyl resonance also has cross-peaks with the isopropyl methyl groups at 1.39 and 1.47 ppm, confirming its assignment as the hydrogen closest to the wedge. The isopropyl methine centered at 3.15 ppm has cross-peaks with the other isopropyl methyl resonances at 1.22 and 1.62 ppm and no NOE enhancement with the zirconium hydride. These resonances are assigned to the substituents on the benzo ring over the zirconocene wedge.

The activation parameters for ring rotation have been extracted from an Eyring plot based on rate constants determined from line shape analysis over a 40 °C temperature range. At certain temperatures, quantitative EXSY NMR experiments were also used as an independent confirmation of the rate data. For example, at  $-54\text{ }^\circ\text{C}$  the EXSY data provided a rate constant of  $31(2)\text{ s}^{-1}$  for ring exchange, statistically invariant from the value of  $34(2)\text{ s}^{-1}$  determined from independent line shape analysis. From these data, values of  $\Delta H^\ddagger = 13.2(3)\text{ kcal/mol}$  and  $\Delta S^\ddagger = 10(3)\text{ eu}$  were determined.

The dynamics of phosphine exchange were also studied using <sup>31</sup>P EXSY NMR spectroscopy. One possibility is that phosphine dissociation is related to the observed ring dynamics. At  $23\text{ }^\circ\text{C}$  and a mixing time of 300 ms, cross-peaks were observed

between free and bound phosphine, indicating rapid exchange under these conditions. Cooling the sample to  $-54\text{ }^\circ\text{C}$  while maintaining a 300 ms mixing time resulted in loss of the exchange peaks, consistent with a static phosphine ligand. Importantly, the <sup>1</sup>H EXSY NMR spectrum at  $-54\text{ }^\circ\text{C}$  (mixing time 250 ms) exhibited cross-peaks between the two indenyl ligands, demonstrating that ring exchange is operative in the static phosphine regime.

Similar solution dynamics were observed with the **PMe<sub>3</sub>** adduct of the silyl-substituted bis(indenyl)zirconium dihydride **1-H<sub>2</sub>(PMe<sub>3</sub>)**. Broadened indenyl ligand peaks were observed by <sup>1</sup>H NMR spectroscopy in toluene-*d*<sub>8</sub> at  $23\text{ }^\circ\text{C}$ . While these resonances sharpen upon cooling to  $-80\text{ }^\circ\text{C}$ , the dynamic process could not be frozen out, indicating that the barrier to ring exchange in this compound is lower than that for **5-H<sub>2</sub>(PMe<sub>3</sub>)**. We have previously examined the variable-temperature NMR behavior of the bis(indenyl)iron sandwich complexes ( $\eta^5\text{-C}_9\text{H}_5\text{-1,3-R}_2$ )<sub>2</sub>Fe ( $R = \text{SiMe}_3, \text{CHMe}_2$ ) and found that the [SiMe<sub>3</sub>]-substituted compound has a higher barrier for ring rotation than the corresponding [CHMe<sub>2</sub>]-substituted derivative.<sup>18</sup>

One notable difference between the two classes of compounds is the ground state conformation of the indenyl rings (Figure 3). For the iron examples, crystallographic studies established a preference for gauche rotamers as the preferred ligand conformation in the solid state.<sup>18</sup> Variable-temperature <sup>1</sup>H NMR studies on the [SiMe<sub>3</sub>]-substituted compound were consistent with geared, synchronous rotations of the rings such that the sterically demanding substituents avoid transannular steric interactions but most likely never fully eclipse.<sup>16,29</sup> When smaller substituents were present, only fast rotation was observed. As a result, the larger the substituents, the higher the barrier to ring rotation.

In the zirconium cases described herein, the presence of a third, neutral ligand in the zirconocene wedge results in a preference for anti conformers, a result of minimizing interactions between the ring substituents and the phosphine ligands. Variable-temperature NMR studies on the bis(indenyl)zirconocene dichloride, dimethyl, and dihydride compounds ( $\eta^5\text{-C}_9\text{H}_5\text{-1,3-R}_2$ )<sub>2</sub>ZrX<sub>2</sub> ( $R = \text{SiMe}_3, \text{CHMe}_2$ ;  $X = \text{Cl, Me, H}$ ) provided no evidence for restricted ring rotation at temperatures as low as  $-80\text{ }^\circ\text{C}$ ,<sup>14,18</sup> further supporting the notion that ligand coordination is the origin of the rotational barriers observed with

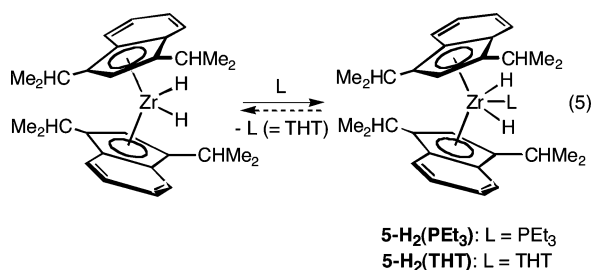
(28) Hillhouse, G. L.; Bulls, A. R.; Santarsiero, B. D.; Bercaw, J. E. *Organometallics* **1988**, *7*, 1309.

(29) (a) Okuda, J.; Herdtweck, E. *Chem. Ber.* **1988**, *121*, 1899. (b) Thornberry, M. P.; Slebonick, C.; Deck, P. A.; Fronczek, F. R. *Organometallics* **2000**, *19*, 5352.

both **5-H<sub>2</sub>(PMe<sub>3</sub>)** and **1-H<sub>2</sub>(PMe<sub>3</sub>)**. Waymouth and co-workers have also found that the identity of the ligands in the zirconocene wedge influence the barriers to ring rotation more so than the indenyl ring substituents.<sup>30,31</sup>

On the basis of the available experimental data, rationalizing the relative rates of ring interconversion as a function of indenyl substituent is not straightforward. Because of the high lipophilicity of **1-H<sub>2</sub>(PMe<sub>3</sub>)**, single crystals were not obtained and, as a result, the conformational preference of the indenyl ligands in the solid state remains unknown. The observed difference in ring exchange barriers may be a result of the relative ground-state energetics of the two compounds. It is possible that the [SiMe<sub>3</sub>]-substituted derivative is sterically destabilized relative to the [CHMe<sub>2</sub>]-substituted compound and, assuming smaller transition state energy differences, would have a lower barrier for ring interchange. However, a different conformational preference in the ground state or ring slippage to an η<sup>3</sup> haptomer in the transition structure cannot be excluded on the basis of the current experimental data.

To gain additional support for restricted ring rotation as the origin of the dynamic process, other principally σ-donating ligands were added to **5-H<sub>2</sub>**. Treatment of the dihydride with PEt<sub>3</sub> resulted in isolation of the phosphine dihydride complex (η<sup>5</sup>-C<sub>9</sub>H<sub>5</sub>-1,3-(CH<sub>2</sub>Me<sub>2</sub>)<sub>2</sub>)<sub>2</sub>ZrH<sub>2</sub>(PEt<sub>3</sub>) (**5-H<sub>2</sub>(PEt<sub>3</sub>)**) as a yellow solid (eq 5). As with the PMe<sub>3</sub> compound, **5-H<sub>2</sub>(PEt<sub>3</sub>)** exhibits

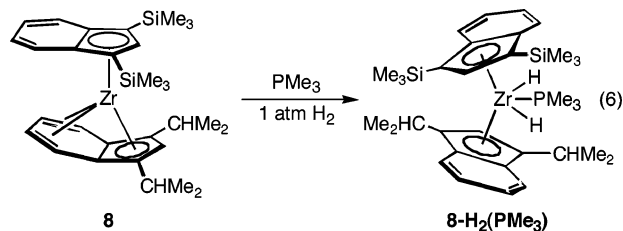


a broadened toluene-*d*<sub>8</sub> <sup>1</sup>H NMR spectrum at 23 °C. Cooling the sample to −54 °C produced a sharp spectrum consistent with a static C<sub>s</sub>-symmetric compound with the phosphine coordinated in the central position of the metallocene wedge. Using line shape analysis, activation parameters of Δ*H*<sup>‡</sup> = 11.3(5) kcal/mol and Δ*S*<sup>‡</sup> = 2(3) eu were extracted from an Eyring plot constructed over a 40 °C temperature range. The free energies of activation (Δ*G*<sup>‡</sup><sub>298</sub>) for **5-H<sub>2</sub>(PMe<sub>3</sub>)** and **5-H<sub>2</sub>(PEt<sub>3</sub>)**, comparable at 10.2(3) and 10.7(5) kcal/mol, respectively, indicate that the slightly larger phosphine, PEt<sub>3</sub>, modestly increases the barrier to ring rotation; however, given the error associated with these measurements, this conclusion is tenuous.

A similar adduct, **5-H<sub>2</sub>(THT)**, was also prepared by addition of 5 equiv of tetrahydrothiophene (THT) to **5-H<sub>2</sub>** (eq 5). Unlike the case for the phosphine compounds, **5-H<sub>2</sub>(THT)** is unstable in the absence of excess ligand, rapidly reverting to **5-H<sub>2</sub>** upon removal of THT. The <sup>1</sup>H NMR spectrum of **5-H<sub>2</sub>(THT)** in toluene-*d*<sub>8</sub> at 23 °C with excess THT exhibits sharp resonances, the number of which are consistent with a C<sub>2v</sub>-symmetric molecule with the THT ligand coordinated in the central position of the metallocene wedge. Cooling the solution to −80 °C produced only a slight change in the spectrum, most notably an upfield shifting of the hydride resonance from 4.58 ppm at

23 °C to 3.05 ppm at the lower temperature. Likewise, the cyclopentadienyl hydrogen migrates from 5.48 to 3.61 ppm upon cooling. Taken together, these data are consistent with an increased concentration of the coordinatively saturated adduct, **5-H<sub>2</sub>(THT)**, at lower temperatures. However, we have been unable to freeze out ring rotation in this complex, consistent with the observed dynamics in the larger phosphine compounds being a result of ring rotation rather than a change in hapticity.

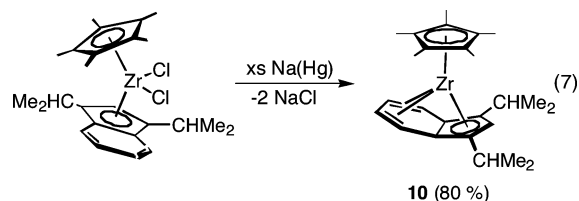
Coordination of PMe<sub>3</sub> was also explored with a “mixed ring” bis(indenyl)zirconocene dihydride. Addition of 1 equiv of phosphine to (η<sup>9</sup>-C<sub>9</sub>H<sub>5</sub>-1,3-(CHMe<sub>2</sub>)<sub>2</sub>)(η<sup>5</sup>-C<sub>9</sub>H<sub>5</sub>-1,3-(SiMe<sub>3</sub>)<sub>2</sub>)-Zr (**8**) followed by exposure to 1 atm of dihydrogen allowed isolation of a yellow solid identified as (η<sup>5</sup>-C<sub>9</sub>H<sub>5</sub>-1,3-(SiMe<sub>3</sub>)<sub>2</sub>)(η<sup>5</sup>-C<sub>9</sub>H<sub>5</sub>-1,3-(CHMe<sub>2</sub>)<sub>2</sub>)ZrH<sub>2</sub>(PMe<sub>3</sub>) (**8-H<sub>2</sub>(PMe<sub>3</sub>)**) (eq 6). The



procedure of first adding phosphine followed by H<sub>2</sub> addition is preferred, as the bis(indenyl)zirconocene dihydride **8-H<sub>2</sub>** undergoes rapid rearrangement at ambient temperature.<sup>16</sup> This synthetic route is effective, as the (η<sup>9</sup>-indenyl)(η<sup>5</sup>-indenyl)-zirconium sandwich complexes do not strongly bind monodentate phosphines.<sup>14</sup>

At 23 °C, the toluene-*d*<sub>8</sub> <sup>1</sup>H NMR spectrum of **8-H<sub>2</sub>(PMe<sub>3</sub>)** exhibits the number of peaks consistent with a C<sub>s</sub>-symmetric complex containing two chemically distinct indenyl rings with PMe<sub>3</sub> coordinated in the central position of the zirconocene wedge. Cooling the solution to −54 °C allowed observation of two isomers (5:1) by <sup>1</sup>H and <sup>31</sup>P NMR spectroscopy. On the basis of NOESY NMR data collected at −54 °C, the major and minor isomers were assigned as two diastereomeric anti rotamers of **8-H<sub>2</sub>(PMe<sub>3</sub>)**. The major isomer (Figure 3) is assigned as the one in which the alkylated indenyl ring orients its benzo substituent over the zirconocene wedge, while the minor is the opposite case, where the silylated indenyl has the six-membered ring over the wedge.

To further explore the possibility of hindered ring rotation rather than a hapticity change as the origin of ring inequivalency, a mixed cyclopentadienyl–indenyl complex was prepared. Treatment of (η<sup>5</sup>-C<sub>5</sub>Me<sub>5</sub>)ZrCl<sub>3</sub><sup>32</sup> with Li[C<sub>9</sub>H<sub>5</sub>-1,3-(CHMe<sub>2</sub>)<sub>2</sub>] furnished the desired zirconocene dichloride complex (η<sup>5</sup>-C<sub>5</sub>Me<sub>5</sub>)(η<sup>5</sup>-C<sub>9</sub>H<sub>5</sub>-1,3-(CHMe<sub>2</sub>)<sub>2</sub>)ZrCl<sub>2</sub> (**10-Cl<sub>2</sub>**). Reduction of this compound with an excess of 0.5% sodium amalgam yielded a red solid identified as the sandwich complex (η<sup>5</sup>-C<sub>5</sub>Me<sub>5</sub>)(η<sup>9</sup>-C<sub>9</sub>H<sub>5</sub>-1,3-(CHMe<sub>2</sub>)<sub>2</sub>)Zr (**10**) (eq 7).



The NMR spectral features of **10** are diagnostic of η<sup>9</sup>-indenyl coordination.<sup>12</sup> Benzo resonances centered at 3.73 and 5.07 ppm and at 65.89 and 96.14 ppm were observed in the benzene-*d*<sub>6</sub>

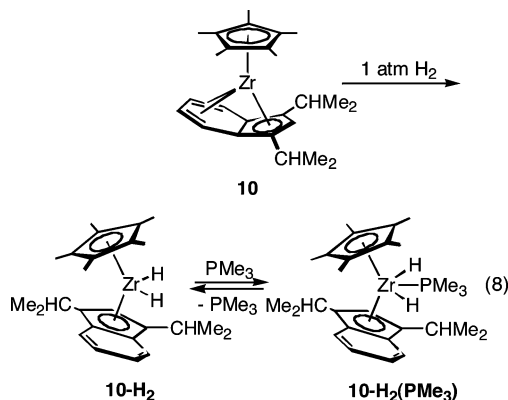
(30) (a) Wilmes, G. M.; France, M. B.; Lynch, S. R.; Waymouth, R. M. *Organometallics* **2004**, *23*, 2405. (b) Lincoln, A. L.; Wilmes, G. M.; Waymouth, R. M. *Organometallics* **2005**, *24*, 5828.

(31) For another study on indenyl conformation dynamics in zirconocene chemistry see: Drier, T.; Bergander, K.; Wegelius, E.; Frölich, R.; Erker, G. *Organometallics* **2001**, *20*, 5067.

(32) Wolczanski, P. T.; Bercaw, J. E. *Organometallics* **1982**, *1*, 793.



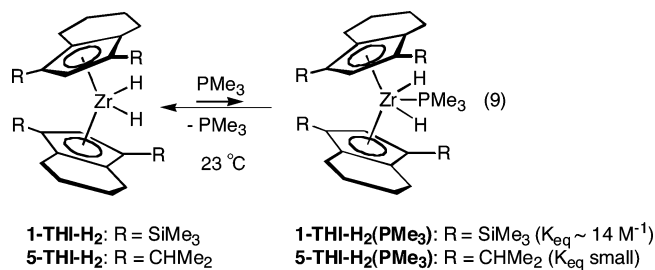
$^1\text{H}$  and  $^{13}\text{C}$  NMR spectra, respectively. Addition of 1 atm of dihydrogen to **10** at 23 °C produced a rapid color change from red to bright yellow. Solvent removal followed by recrystallization from pentane furnished a yellow solid identified as  $(\eta^5\text{-C}_5\text{Me}_5)(\eta^5\text{-C}_9\text{H}_5\text{-1,3-(CHMe}_2)_2)\text{ZrH}_2$  (**10-H<sub>2</sub>**) (eq 8). As with



the bis(indenyl)zirconocene dihydrides, a downfield zirconium hydride resonance centered at 7.27 ppm was observed in the ambient-temperature benzene- $d_6$   $^1\text{H}$  NMR spectrum, indicative of a monomeric species in solution.<sup>33</sup>

Addition of an excess (~18 equiv) of  $\text{PMe}_3$  to a toluene- $d_8$  solution of **10-H<sub>2</sub>** at 23 °C resulted in complete conversion to the phosphine adduct  $(\eta^5\text{-C}_5\text{Me}_5)(\eta^5\text{-C}_9\text{H}_5\text{-1,3-(CHMe}_2)_2)\text{ZrH}_2(\text{PMe}_3)$  (**10-H<sub>2</sub>(PMe<sub>3</sub>)**), as judged by  $^1\text{H}$  NMR spectroscopy. If fewer equivalents of  $\text{PMe}_3$  are added, an equilibrium between the dihydride and the adduct was observed. Accordingly, exposure of a benzene- $d_6$  solution containing **10-H<sub>2</sub>(PMe<sub>3</sub>)** and excess phosphine to vacuum resulted in regeneration of the dihydride **10-H<sub>2</sub>**. The  $^1\text{H}$  NMR spectrum of **10-H<sub>2</sub>(PMe<sub>3</sub>)** at 23 °C in the presence of phosphine exhibits sharp ligand resonances consistent with a  $C_s$ -symmetric compound with a  $\text{PMe}_3$  ligand coordinated in the central position of the metallocene wedge. Notably, a broad singlet centered at 2.18 ppm for the zirconium hydride resonances was observed at 23 °C, consistent with rapid dissociation and recoordination of the phosphine on the NMR time scale. Cooling the solution to -70 °C produced a well-resolved doublet ( $^3J_{\text{P-H}} = 69$  Hz) shifted slightly upfield to 2.09 ppm, consistent with a static bound phosphine. The cyclopentadienyl hydrogens appear at 4.84 and 4.87 ppm at 23 and -70 °C, respectively. These resonances appear downfield as compared to those for the other bis(indenyl)zirconium dihydride phosphine adducts, supporting transannular ring currents as the origin of the upfield shifts. Significantly, the  $^{13}\text{C}$  NMR chemical shift of the ring junction carbon was observed at 117.14 ppm (Table 3), a value comparable to that for the free indenide ligand and the shifts measured for **1-H<sub>2</sub>(PMe<sub>3</sub>)**, consistent with  $\eta^5$  coordination upon complexation of the phosphine ligand.

To determine if there was an “indenyl effect” influencing ligand coordination, similar binding studies were conducted with the bis(tetrahydroindenyl)zirconium dihydrides **1-THI-H<sub>2</sub>** and **5-THI-H<sub>2</sub>**. Addition of 5 equiv of  $\text{PMe}_3$  (0.0837 M) to a benzene- $d_6$  solution of **1-THI-H<sub>2</sub>** produced two broadened resonances in the  $^{31}\text{P}$  NMR spectrum at -54 °C, consistent with free and coordinated phosphine (eq 9). Integration of these resonances established an equilibrium constant ( $K_{\text{eq}}$ ) of 14(2)  $\text{M}^{-1}$  at -54 °C. Warming the sample to ambient temperature or exposure to vacuum resulted in clean and quantitative



regeneration of **1-THI-H<sub>2</sub>**. Performing a similar experiment with the alkyl-substituted dihydride **5-THI-H<sub>2</sub>** and approximately 17 equiv of  $\text{PMe}_3$  produced no reaction at temperatures between 23 and -80 °C.

Because no change in hapticity is observed upon ligand coordination to the bis(indenyl)zirconocene dihydride compounds, the differences in the thermodynamics for ligand coordination are most likely a result of the increased electrophilicity of the indenyl-substituted zirconocenes. Within a similar ligand class (e.g. indenyl versus tetrahydroindenyl), substituents can play a role, with more electron withdrawing silyl substituents favoring both olefin insertion and ligand coordination processes. In the mixed cyclopentadienyl-indenyl compound, introduction of an electron-donating pentamethylcyclopentadienyl ligand also decreases the affinity for  $\text{PMe}_3$  coordination.

## Concluding Remarks

The “indenyl effect” as it pertains to group 4 zirconocene dihydride chemistry has been evaluated through a study of olefin insertion rates and binding constants for addition of  $\sigma$ -donating ligands. Complexes bearing indenyl substituents undergo cyclohexene insertion much more quickly and have a higher affinity for exogenous ligands than their tetrahydroindenyl counterparts. While the solid-state structure of a bis(indenyl)zirconium dihydride phosphine adduct demonstrates a slight deviation from typical  $\eta^5$  hapticity, the indenyl effect observed in this study is primarily a result of the increased electrophilicity of the metal center, rather than a distinct change in hapticity from  $\eta^5$  to  $\eta^3$  coordination along the reaction coordinate.

## Experimental Section

**General Considerations.** All air- and moisture-sensitive manipulations were carried out using standard vacuum-line, Schlenk, or cannula techniques or in an M. Braun inert-atmosphere drybox containing an atmosphere of purified nitrogen. Solvents for air- and moisture-sensitive manipulations were initially dried and deoxygenated using literature procedures.<sup>34</sup> Benzene- $d_6$  and toluene- $d_8$  for NMR spectroscopy were distilled from sodium metal under an atmosphere of argon and stored over 4 Å molecular sieves or sodium metal. Trimethylphosphine was purchased from Strem and was dried over molecular sieves before use. Triethylphosphine was purchased from Aldrich and dried over sieves prior to use. Tetrahydrothiophene was purchased from Acros and dried over calcium hydride prior to use. Hydrogen was purchased from Airgas, while deuterium was purchased from Cambridge Isotope Laboratories; both were passed through a drying column packed with  $\text{MnO}_2$  and 4 Å molecular sieves before use. **1**, **5**, **8**, **1-H<sub>2</sub>**, **5-H<sub>2</sub>**, **8-H<sub>2</sub>**, **1-THI-H<sub>2</sub>**, and **5-THI-H<sub>2</sub>** were prepared according to literature procedures.<sup>11,12,16</sup> All calibrated gas bulb experiments were conducted using a 100.1 mL bulb unless noted otherwise.

(33) Chirik, P. J.; Day, M. W.; Bercaw, J. E. *Organometallics* **1999**, *18*, 1873.

(34) Pangborn, A. B.; Giardello, M. A.; Grubbs, R. H.; Rosen, R. K.; Timmers, F. J. *Organometallics* **1996**, *15*, 1518.

$^1\text{H}$  and  $^{13}\text{C}$  NMR spectra were recorded on a Varian Inova 400 spectrometer operating at 399.779 MHz ( $^1\text{H}$ ) and 110.524 MHz ( $^{13}\text{C}$ ). All chemical shifts are reported relative to  $\text{SiMe}_4$  using  $^1\text{H}$  (residual) or  $^{13}\text{C}$  NMR chemical shifts of the solvent as a secondary standard.  $^{31}\text{P}$  NMR spectra were externally referenced relative to 85%  $\text{H}_3\text{PO}_4$  in water.  $^2\text{H}$  NMR spectra were recorded on a Varian Inova 500 spectrometer operating at 76.740 MHz, and the spectra were referenced using an internal benzene- $d_6$  standard. Variable-temperature (VT) and two-dimensional NMR experiments were performed on a Varian Inova 500 spectrometer operating at 499.920 MHz for  $^1\text{H}$  and 125.704 MHz for  $^{13}\text{C}$ . The temperature for the VT experiments was calibrated using methanol and ethylene glycol standards. Line shape analyses were performed using DNMR as implemented by Spinworks 2.2.<sup>35</sup>

Qualitative EXSY spectra were acquired with a sweep width of 1.8 kHz and a mixing time of 200 ms in phase-sensitive mode. For quantitative rate studies, mixing times of 300, 200, 100, 50, and 0 ms were used at a temperature of  $-54\text{ }^\circ\text{C}$ . Cross-peak integration was performed in Mest-Rec C;<sup>36</sup> intensities were normalized and rates were calculated using EXSY Calc.<sup>37</sup> A total of 64 complex points were collected in the indirectly detected dimension with 8 scans and 1k points per increment. The resulting matrix was zero-filled to  $2\text{k} \times 2\text{k}$  complex data points, and 90 shifted squared sinusoidal window functions were applied in both dimensions prior to Fourier transform. Unless otherwise noted, all other two-dimensional spectra were recorded at  $-54\text{ }^\circ\text{C}$  using parameters described previously.<sup>14</sup>

Single crystals suitable for X-ray diffraction were coated with polyisobutylene oil in a drybox, transferred to a nylon loop, and then quickly transferred to the goniometer head of a Bruker X8 APEX2 diffractometer equipped with a molybdenum X-ray tube ( $\lambda = 0.71073\text{ \AA}$ ). Preliminary data revealed the crystal system. A hemisphere routine was used for data collection and determination of lattice constants. The space group was identified, and the data were processed using the Bruker SAINT+ program and corrected for absorption using SADABS. The structures were solved using direct methods (SHELXS) completed by subsequent Fourier synthesis and refined by full-matrix least-squares procedures. Elemental analyses were performed at Robertson Microlit Laboratories, Inc., in Madison, NJ.

**Preparation of  $(\eta^5\text{-C}_9\text{H}_5\text{-1,3-(SiMe}_3)_2)_2\text{ZrH}_2(\text{PMe}_3)$  (**1-H}\_2(\text{PMe}\_3)**).** A thick-walled glass vessel was charged with 0.100 g (0.16 mmol) of **1** and approximately 5 mL of pentane. The vessel was sealed, removed from the drybox, submerged in liquid nitrogen, and degassed on a vacuum line. One atmosphere of hydrogen was added at liquid-nitrogen temperature, the vessel was sealed and warmed to ambient temperature, and the resulting reaction mixture was stirred for 5 min. The vessel was again submerged in liquid nitrogen, and 36 Torr (0.20 mmol) of  $\text{PMe}_3$  was added via a calibrated gas volume. The reaction mixture was warmed to ambient temperature and stirred for 15 min, after which time the solvent was removed in vacuo, yielding 0.092 g (82%) of a yellow oil identified as **1-H}\_2(\text{PMe}\_3)**.  $^1\text{H}$  NMR (toluene- $d_8$ ,  $-54\text{ }^\circ\text{C}$ ):  $\delta$  0.45 (s, 36H,  $\text{SiMe}_3$ ), 1.22 (br s, 9H,  $\text{PMe}_3$ ), 1.76 (d, 72 Hz, 2H, Zr-H), 4.88 (s, 2H, Cp), 6.66 (br, 4H, benzo), 7.25 (br, 4H, benzo).  $^{13}\text{C}$  NMR (toluene- $d_8$ ,  $-54\text{ }^\circ\text{C}$ ):  $\delta$  2.37 ( $\text{SiMe}_3$ ), 24.12 (d, 16 Hz,  $\text{PMe}_3$ ), 101.90, 114.19, 122.19, 122.42, 124.55 (Cp/benzo).  $^{31}\text{P}\{^1\text{H}\}$  NMR (toluene- $d_8$ ,  $-54\text{ }^\circ\text{C}$ ):  $\delta$   $-13.79$ .

**Preparation of  $(\eta^5\text{-C}_9\text{H}_5\text{-1,3-(CHMe}_2)_2)_2\text{ZrH}_2(\text{PMe}_3)$  (**5-H}\_2(\text{PMe}\_3)**).** This molecule was prepared in a manner similar to that for **1-H}\_2(\text{PMe}\_3)**, using 0.110 g (0.22 mmol) of **5** and 40 Torr (0.22

mmol) of  $\text{PMe}_3$ , yielding 0.042 g (33%) of **5-H}\_2(\text{PMe}\_3)**. Anal. Calcd for  $\text{C}_{33}\text{H}_{49}\text{ZrP}$ : C, 70.03; H, 8.37. Found: C, 69.79; H, 8.70.  $^1\text{H}$  NMR (toluene- $d_8$ ,  $23\text{ }^\circ\text{C}$ ):  $\delta$  0.80 (br, 9H,  $\text{PMe}_3$ ), 1.36 (d, 8 Hz, 12H,  $\text{CHMe}_2$ ), 1.41 (d, 8 Hz, 12H,  $\text{CHMe}_2$ ), 2.33 (d, 70 Hz, 2H, Zr-H), 3.38 (br, 4H,  $\text{CHMe}_2$ ), 3.55 (br, 2H, Cp), 6.69 (m, 4H, benzo), 7.46 (m, 4H, benzo).  $^1\text{H}$  NMR (toluene- $d_8$ ,  $-54\text{ }^\circ\text{C}$ ):  $\delta$  0.83 (d, 6 Hz, 9H,  $\text{PMe}_3$ ), 1.21 (br, 6H,  $\text{CHMe}_2$ ), 1.38 (br, 6H,  $\text{CHMe}_2$ ), 1.47 (br, 6H,  $\text{CHMe}_2$ ), 1.64 (br, 6H,  $\text{CHMe}_2$ ), 2.24 (d, 69 Hz, 2H, Zr-H), 2.76 (s, 1H, Cp), 3.14 (br, 1H,  $\text{CHMe}_2$ ), 3.86 (br, 1H,  $\text{CHMe}_2$ ), 4.47 (s, 1H, Cp), 6.65 (br, 2H, benzo), 6.83 (br, 2H, benzo), 7.48 (m, 4H, benzo).  $^{13}\text{C}$  NMR (toluene- $d_8$ ,  $-54\text{ }^\circ\text{C}$ ):  $\delta$  23.88, 25.78, 26.10, 26.49, 28.87, 29.30 ( $\text{CHMe}_2$ ), 99.67, 111.59, 116.14, 118.54, 120.39, 121.29, 121.68, 124.46 (Cp/benzo). The  $\text{PMe}_3$  and two Cp/benzo resonances were not located.  $^{31}\text{P}\{^1\text{H}\}$  NMR (toluene- $d_8$ ,  $-54\text{ }^\circ\text{C}$ ):  $\delta$   $-18.67$ .

**Preparation of  $(\eta^5\text{-C}_9\text{H}_5\text{-1,3-(CMe}_2\text{H}_2)_2)_2\text{ZrH}_2(\text{PEt}_3)$  (**5-H}\_2(\text{PEt}\_3)**).** This molecule was prepared in a manner similar to that for **1-H}\_2(\text{PMe}\_3)** with 0.075 g (0.15 mmol) of **5** and 31 Torr (0.17 mmol) of  $\text{PEt}_3$ , yielding 0.025 g (27%) of **5-H}\_2(\text{PEt}\_3)** as yellow crystals. Anal. Calcd for  $\text{C}_{33}\text{H}_{55}\text{ZrP}$ : C, 70.88; H, 9.09. Found: C, 70.96; H, 8.83.  $^1\text{H}$  NMR (toluene- $d_8$ ,  $23\text{ }^\circ\text{C}$ ):  $\delta$  0.96 (t, 8 Hz, 9H,  $\text{PEt}_3$ ), 1.18 (m, 6H,  $\text{PEt}_3$ ), 1.27 (br, 12H,  $\text{CHMe}_2$ ), 1.40 (br, 12H,  $\text{CHMe}_2$ ), 3.12 (br, 4H,  $\text{CHMe}_2$ ), 6.74 (m, 4H, benzo), 7.29 (br, 4H, benzo). The Zr-H and Cp hydrogens were not located.  $^1\text{H}$  NMR (toluene- $d_8$ ,  $-70\text{ }^\circ\text{C}$ ):  $\delta$  1.02 (br, 9H,  $\text{PEt}_3$ ), 1.18 (m, 6H,  $\text{PEt}_3$ ), 1.28 (br, 6H,  $\text{CHMe}_2$ ), 1.37 (br, 6H,  $\text{CHMe}_2$ ), 1.47 (br, 6H,  $\text{CHMe}_2$ ), 1.82 (br, 6H,  $\text{CHMe}_2$ ), 2.44 (d, 67 Hz, 2H, Zr-H), 2.54 (s, 1H, Cp), 3.09 (br, 2H,  $\text{CHMe}_2$ ), 3.84 (br, 2H,  $\text{CHMe}_2$ ), 4.34 (s, 1H, Cp), 6.56 (br, 2H, benzo), 6.83 (br, 2H, benzo), 7.42 (m, 2H, benzo), 7.46 (m, 2H, benzo).  $^{13}\text{C}$  NMR (toluene- $d_8$ ,  $-70\text{ }^\circ\text{C}$ ):  $\delta$  16.26 ( $\text{PEt}_3$ ), 19.03 ( $\text{PEt}_3$ ), 23.33, 25.52, 26.54, 29.04, 29.46 ( $\text{CHMe}_2$ ), 99.53, 112.84, 115.90, 116.44, 118.38, 120.36, 121.35, 121.73, 124.67, 124.99 (Cp/benzo). One  $\text{CHMe}_2$  resonance not located.  $^{31}\text{P}\{^1\text{H}\}$  NMR (toluene- $d_8$ ,  $-54\text{ }^\circ\text{C}$ ):  $\delta$  16.08.

**Spectroscopic Identification of  $(\eta^5\text{-C}_9\text{H}_5\text{-1,3-(CHMe}_2)_2)_2\text{ZrH}_2(\text{THT})$  (**5-H}\_2(\text{THT})**).** This molecule was prepared in a manner similar to that for **1-H}\_2(\text{PMe}\_3)**, using 0.015 g (0.031 mmol) of **5** and 36 Torr (0.15 mmol) of THT.  $^1\text{H}$  NMR (toluene- $d_8$ ,  $23\text{ }^\circ\text{C}$ , 5 equiv of THT):  $\delta$  1.29 (d, 7 Hz, 12H,  $\text{CHMe}_2$ ), 1.34 (d, 7 Hz, 12H,  $\text{CHMe}_2$ ), 3.15 (m, 4H,  $\text{CHMe}_2$ ), 4.58 (br, 2H, Zr-H), 5.48 (br, 2H, Cp), 6.71 (m, 4H, benzo), 7.26 (m, 4H, benzo). The THT resonances were not located.  $^{13}\text{C}$  NMR (toluene- $d_8$ ,  $23\text{ }^\circ\text{C}$ , 5 equiv of THT):  $\delta$  23.57, 26.10, 27.98, 31.65, 33.07 ( $\text{CHMe}_2$ ), 109.82, 119.75, 120.59, 121.80, 124.99 (Cp/benzo). One  $\text{CHMe}_2$  and two THT resonances were not located.  $^1\text{H}$  NMR (toluene- $d_8$ ,  $-80\text{ }^\circ\text{C}$ , 5 equiv of THT):  $\delta$  1.26 (br, 4H, THT), 1.52 (br, 12H,  $\text{CHMe}_2$ ), 1.57 (br, 12H,  $\text{CHMe}_2$ ), 2.37 (br, 4H, THT), 3.05 (s, 2H, Zr-H), 3.61 (br, 6H, Cp/ $\text{CHMe}_2$ ), 6.68 (br, 4H, benzo), 7.49 (br, 2H, benzo). One Cp/ $\text{CHMe}_2$  resonance not found.  $^{13}\text{C}$  NMR (toluene- $d_8$ ,  $-80\text{ }^\circ\text{C}$ , 5 equiv of THT):  $\delta$  24.50, 26.06, 29.13, 40.64 (THT/ $\text{CHMe}_2$ ), 117.57, 121.22, 124.41, 124.45 (Cp/benzo). One THT/ $\text{CHMe}_2$  and one Cp/benzo resonance were not located.

**Preparation of  $(\eta^5\text{-C}_9\text{H}_5\text{-1,3-(SiMe}_3)_2)(\eta^5\text{-C}_9\text{H}_5\text{-1,3-(CHMe}_2)_2)_2\text{ZrH}_2(\text{PMe}_3)$  (**8-H}\_2(\text{PMe}\_3)**).** A thick-walled glass vessel was charged with 0.132 g (0.24 mmol) of **8** and approximately 10 mL of pentane. The contents of the vessel were frozen in liquid nitrogen, the vessel was evacuated, and 49 Torr (0.26 mmol) of  $\text{PMe}_3$  was added by calibrated volume. The contents of the vessel were warmed to room temperature, and the resulting solution was stirred for approximately 15 min. The contents of the vessel were again frozen in liquid nitrogen, the vessel was evacuated, and 1 atm of dihydrogen was admitted. The reaction mixture was warmed to ambient temperature and stirred for 5 min. Solvent removal followed by extraction and recrystallization from pentane yielded 0.061 g (41%) of a yellow solid identified as **8-H}\_2(\text{PMe}\_3)**. Anal. Calcd for  $\text{C}_{33}\text{H}_{53}\text{Si}_2\text{ZrP}$ : C, 63.10; H, 8.51. Found: C, 63.27; H, 8.28.  $^1\text{H}$  NMR (benzene- $d_6$ ,  $23\text{ }^\circ\text{C}$ ):  $\delta$  0.49 (s, 18H,  $\text{SiMe}_3$ ), 0.81 (br, 9H,

(35) Marat, K. Spinworks; University of Manitoba, 2004.

(36) Gómez, J. C. C.; López, F. J. S. MestRe-C, version 3.7.1.9.0; Universidade de Santiago de Compostela, 2004, www.mestrec.com.

(37) (a) Perrin, C. L.; Dwyer, T. J. *Chem. Rev.* **1990**, *90*, 935. (b) Derose, E. F.; Castillo, J.; Saulys, D.; Morrison, J. J. *Magn. Reson.* **1991**, *93*, 347. (c) Zolnai, Z.; Juranic, N.; Vikić-Topić, D.; Macura, S. *J. Chem. Inf. Comput. Sci.* **2000**, *40*, 611.



$\text{PMe}_3$ ), 1.35 (br, 12H,  $\text{CHMe}_2$ ), 2.33 (d, 68 Hz, 2H, Zr-H), 3.72 (br, 2H, Cp/ $\text{CHMe}_2$ ), 4.37 (br, 2H Cp/ $\text{CHMe}_2$ ), 6.73 (br, 4H, benzo), 7.51 (br, 4H, benzo).  $^1\text{H}$  NMR (toluene- $d_8$ ,  $-54^\circ\text{C}$ ): major,  $\delta$  0.54 (s, 18H,  $\text{SiMe}_3$ ), 0.81 (br s, 9H,  $\text{PMe}_3$ ), 1.16 (d, 6 Hz, 6H,  $\text{CHMe}_2$ ), 1.47 (d, 6 Hz, 6H,  $\text{CHMe}_2$ ), 2.31 (d, 73 Hz, 2H, Zr-H), 3.26 (s, 1H, Cp), 3.88 (br, 2H,  $\text{CHMe}_2$ ), 4.37 (s, 1H, Cp), 6.60 (br, 2H, benzo), 6.84 (br, 2H, benzo), 7.44 (br, 4H, benzo); minor,  $\delta$  0.49 (s, 18H,  $\text{SiMe}_3$ ), 1.21 (d, 6 Hz, 6H,  $\text{CHMe}_2$ ), 1.80 (d, 6 Hz, 6H,  $\text{CHMe}_2$ ), 2.10 (d, 74 Hz, 2H, Zr-H), 2.47 (s, 1H, Cp), 3.13 (m, 2H,  $\text{CHMe}_2$ ), 4.56 (s, 1H, Cp), 6.69 (br, 2H, benzo), 6.89 (br, 2H, benzo). One  $\text{PMe}_3$  and two benzo resonances were not located.  $^{13}\text{C}\{^31\text{P}\}$  NMR (toluene- $d_8$ ,  $-54^\circ\text{C}$ ): major,  $\delta$  3.20 ( $\text{SiMe}_3$ ), 23.55 ( $\text{PMe}_3$ ), 23.82, 26.45, 29.13 ( $\text{CHMe}_2$ ), 99.81, 104.83, 115.92, 118.34, 122.05, 122.34, 124.77, 126.05, 130.09 (Cp/benzo), One Cp/benzo resonance was not located.  $^{31}\text{P}\{^1\text{H}\}$  NMR (toluene- $d_8$ ,  $-54^\circ\text{C}$ ): major,  $\delta$   $-19.88$ ; minor,  $\delta$   $-18.49$ .

**Spectroscopic Identification of  $(\eta^5\text{-C}_9\text{H}_9\text{-1,3-(SiMe}_3)_2\text{)ZrH}_2\text{(PMe}_3\text{)}$  (**1-THI-H}\_2\text{(PMe}\_3\text{)}**).** A J. Young NMR tube was charged with 0.020 g (0.033 mmol) of **1-THI-H}\_2**, and approximately 0.5 mL of toluene- $d_8$  was added. The tube was attached to a high-vacuum line, the contents were frozen, the tube was evacuated, and 104 Torr (0.56 mmol) of  $\text{PMe}_3$  was added.  $^1\text{H}$  NMR (toluene- $d_8$ ,  $-54^\circ\text{C}$ ):  $\delta$  0.28 (s, 36H,  $\text{SiMe}_3$ ), 1.71 (br, 4H, THI), 2.01 (br, 4H, THI), 2.65 (m, 4H, THI), 2.76 (m, 4H, THI), 5.38 (br s, 2H, Zr-H), 5.55 (s, 2H, Cp).  $^{13}\text{C}$  NMR (toluene- $d_8$ ,  $-54^\circ\text{C}$ ):  $\delta$  1.91 ( $\text{SiMe}_3$ ), 24.42, 27.98 (THI), 112.28, 116.91, 135.80 (Cp). The  $\text{PMe}_3$  resonance was not located.  $^{31}\text{P}\{^1\text{H}\}$  NMR (toluene- $d_8$ ,  $-54^\circ\text{C}$ ):  $\delta$   $-21.68$ .

**General Procedure for Kinetic Measurements.** A flame dried J. Young NMR tube was charged with 300  $\mu\text{L}$  of a stock solution ( $\sim 0.02$  M) of the desired zirconocene complex and 100  $\mu\text{L}$  of a 0.031 M solution containing sublimed ferrocene. Both solutions were prepared in benzene- $d_6$  or toluene- $d_8$ , depending on the temperature required for data acquisition. The tube containing the stock solution was then attached to a high-vacuum line, and 12 equiv of cyclohexene (0.253 M) was added via a calibrated gas volume at liquid-nitrogen temperature. The tube was transferred into a precooled NMR probe, and the disappearance of starting material and the appearance of product were monitored in an arrayed  $^1\text{H}$  NMR experiment. For slower reactions, the tubes were stored in temperature-controlled water baths and spectra were collected periodically. Spectra were integrated versus the ferrocene standard.

**Spectroscopic Identification of  $(\eta^5\text{-C}_9\text{H}_5\text{-1,3-(SiMe}_3)_2\text{)Zr-(C}_6\text{H}_{11}\text{)H}$  (**1-(Cy)H**).** A J. Young NMR tube was charged with 0.018 g (0.029 mmol) of **1** and dissolved in toluene- $d_8$ . **1-H}\_2** was then generated as described previously,<sup>16</sup> and 65 Torr (0.35 mmol) of cyclohexene was added. The frozen solution was then transferred to a dry ice/acetone bath and quickly inserted into a precooled NMR probe at  $-43^\circ\text{C}$ . After approximately 45 min,  $>90\%$  conversion to **1-(Cy)H** was observed.  $^1\text{H}$  NMR (toluene- $d_8$ ,  $-43^\circ\text{C}$ ):  $\delta$   $-2.75$  (br, 1H, ZrCH), 0.38 (s, 9H,  $\text{SiMe}_3$ ), 0.45 (s, 18H,  $\text{SiMe}_3$ ), 0.49 (s, 9H,  $\text{SiMe}_3$ ), 0.83 (br, 2H, c-hexyl), 0.92 (br, 2H, c-hexyl), 1.04 (br, 1H, c-hexyl), 1.18 (br, 1H, c-hexyl), 1.27 (br, 2H, c-hexyl), 1.76 (br, 2H, c-hexyl), 6.10 (s, 2H, Cp), 6.82 (br, 4H, benzo), 7.24 (br, 1H, benzo), 7.48 (br, 2H, benzo), 7.62 (br, 1H, benzo). The Zr-H resonance was not located.

**Spectroscopic Identification of  $(\eta^5\text{-C}_9\text{H}_5\text{-1,3-(CHMe}_2)_2\text{)Zr-(C}_6\text{H}_{11}\text{)H}$  (**5-(Cy)H**).** This compound was observed in a manner similar to that used for **1-(Cy)H**.  $^1\text{H}$  NMR (toluene- $d_8$ ,  $-43^\circ\text{C}$ ):  $\delta$   $-2.33$  (br, 1H, c-hexyl), 0.92 (br, 4H, c-hexyl), 1.13 (br, 4H, c-hexyl), 1.25 (br, 12H,  $\text{CHMe}_2$ ), 1.36 (br, 6H,  $\text{CHMe}_2$ ), 1.43 (br, 6H,  $\text{CHMe}_2$ ), 1.85 (br, 2H, c-hexyl), 3.22 (br, 2H,  $\text{CHMe}_2$ ), 3.40 (br, 2H,  $\text{CHMe}_2$ ), 6.17 (s, 2H, Cp), 6.79 (s, 1H, Zr-H), 6.87 (br, 4H, benzo), 7.33 (br, 2H, benzo), 7.42 (br, 2H, benzo).

**Spectroscopic Identification of  $(\eta^5\text{-C}_9\text{H}_9\text{-1,3-(SiMe}_3)_2\text{)Zr-(C}_6\text{H}_{11}\text{)H}$  (**1-THI-(Cy)H**).** A J. Young NMR tube was charged with 0.017 g (0.027 mmol) of **1-THI-H}\_2**, which was dissolved in

benzene- $d_6$ . The contents of the tube were frozen, the tube was degassed, and 61 Torr (0.32 mmol) of cyclohexene was added. The resulting reaction mixture was allowed to stand at ambient temperature for 24 h, and the solvent was removed in vacuo. Redissolving the foam in benzene- $d_6$  allowed observation of **1-THI-(Cy)H**.  $^1\text{H}$  NMR (benzene- $d_6$ ,  $23^\circ\text{C}$ ):  $\delta$   $-3.80$  (m, 1H, c-hexyl), 0.29 (s, 18H,  $\text{SiMe}_3$ ), 0.38 (s, 18H,  $\text{SiMe}_3$ ), 0.89 (br, 1H, c-hexyl), 1.18 (br, 1H, c-hexyl), 1.32 (br, 2H, c-hexyl), 1.60–1.70 (br, 6H, THI/c-hexyl), 1.73 (br, 3H, THI/c-hexyl), 2.44 (m, 2H, THI), 2.58 (m, 2H, THI), 2.69 (m, 2H, THI), 2.82 (m, 2H, THI), 5.72 (s, 2H, Cp), 6.02 (s, 1H, Zr-H). Five THI/c-hexyl resonances were not located.  $^{13}\text{C}$  NMR (benzene- $d_6$ ,  $23^\circ\text{C}$ ):  $\delta$  1.92, 1.96 ( $\text{SiMe}_3$ ), 22.79, 23.17, 23.85, 24.19, 27.42, 27.56, 28.10, 28.61 (THI/c-hexyl), 115.19, 123.44, 124.26, 125.55, 136.83 (Cp).

**Spectroscopic Identification of  $(\eta^5\text{-C}_9\text{H}_9\text{-1,3-(CHMe}_2)_2\text{)Zr-(C}_6\text{H}_{11}\text{)H}$  (**5-THI-(Cy)H**).** This molecule was prepared in a manner similar to that described for the observation of **1-THI-(Cy)H**.  $^1\text{H}$  NMR (benzene- $d_6$ ,  $23^\circ\text{C}$ ):  $\delta$  1.13 (d, 7 Hz, 6H,  $\text{CHMe}_2$ ), 1.20 (d, 7 Hz, 6H,  $\text{CHMe}_2$ ), 1.28 (d, 7 Hz, 6H,  $\text{CHMe}_2$ ), 1.32 (d, 7 Hz, 6H,  $\text{CHMe}_2$ ), 1.74 (m, 3H, c-hexyl), 2.05 (m, 3H, c-hexyl), 2.18 (m, 2H, c-hexyl), 2.24 (m, 2H, THI), 2.48 (m, 4H, THI), 2.68 (m, 4H, THI), 2.64 (m, 1H,  $\text{CHMe}_2$ ), 3.09 (m, 1H,  $\text{CHMe}_2$ ), 5.20 (s, 2H, Cp), 5.33 (s, 1H, Zr-H). Three c-hexyl and six THI resonances were not located.

**Preparation of  $(\eta^5\text{-C}_9\text{H}_5\text{-1,3-(CHMe}_2)_2\text{)(}\eta^5\text{-C}_5\text{Me}_5\text{)ZrCl}_2$  (**10-Cl}\_2\text{}**).** A 250 mL round-bottomed flask was charged with 1.50 g (4.51 mmol) of  $(\eta^5\text{-C}_5\text{Me}_5\text{)ZrCl}_3$ , and 100 mL of diethyl ether was added. The solution was chilled in the drybox cold well for 20 min, and 0.930 g (4.51 mmol) of  $[\text{Li}(\text{C}_9\text{H}_5\text{-1,3-(CHMe}_2)_2)]$  was added over 10 min. The reaction was warmed to room temperature and stirred overnight. Upon vacuum removal of solvent, the remaining solid was rinsed with cold pentane and collected on a frit containing Celite. The yellow solid was then rinsed with approximately 75 mL of dichloromethane. Vacuum removal of solvent yielded 1.25 g (56%) of a yellow solid identified as **10-Cl}\_2**. Anal. Calcd for  $\text{C}_{25}\text{H}_{34}\text{ZrCl}_2$ : C, 60.46; H, 6.90. Found: C, 59.83; H, 6.75.  $^1\text{H}$  NMR (benzene- $d_6$ ):  $\delta$  1.06 (d, 6 Hz, 6H,  $\text{CHMe}_2$ ), 1.46 (d, 6 Hz, 6H,  $\text{CHMe}_2$ ), 1.66 (s, 15H,  $\text{C}_5\text{Me}_5$ ), 3.57 (m, 2H,  $\text{CHMe}_2$ ), 6.84 (m, 2H, benzo), 6.87 (s, 1H, Cp), 7.37 (m, 2H, benzo).  $^{13}\text{C}$  NMR (benzene- $d_6$ ):  $\delta$  12.19 ( $\text{C}_5\text{Me}_5$ ), 21.30, 25.72, 27.41 ( $\text{CHMe}_2$ ), 95.49, 123.26, 124.21, 124.31, 125.00, 125.16 (Cp/benzo).

**Preparation of  $(\eta^9\text{-C}_9\text{H}_5\text{-1,3-(CHMe}_2)_2\text{)(}\eta^5\text{-C}_5\text{Me}_5\text{)Zr}$  (**10**).** A 100 mL round-bottomed flask was charged with 15.75 g of mercury, and approximately 10 mL of pentane was added. To the stirred solution was added 0.080 g (3.44 mmol) of sodium, and the vessel was stirred for 20 min to ensure amalgamation. A pentane slurry ( $\sim 10$  mL) containing 0.285 g (0.574 mmol) of **10-Cl}\_2** was then added, an additional 10 mL of pentane was added, and the reaction mixture was stirred vigorously for 24 h. Filtration of the red solution through Celite followed by solvent removal in vacuo produced a red foam. Recrystallization from pentane at  $-35^\circ\text{C}$  yields 0.196 g (80%) of **10** as a red solid. Anal. Calcd for  $\text{C}_{25}\text{H}_{34}\text{Zr}$ : C, 70.52; H, 8.05. Found: C, 70.29; H, 8.40.  $^1\text{H}$  NMR (benzene- $d_6$ ):  $\delta$  1.11 (d, 7 Hz, 6H,  $\text{CHMe}_2$ ), 1.15 (d, 7 Hz, 6H,  $\text{CHMe}_2$ ), 1.80 (s, 15H,  $\text{C}_5\text{Me}_5$ ), 3.22 (m, 2H,  $\text{CHMe}_2$ ), 3.73 (m, 2H, benzo), 5.07 (m, 2H, benzo), 5.86 (s, 1H, Cp).  $^{13}\text{C}$  NMR (benzene- $d_6$ ):  $\delta$  11.97 ( $\text{C}_5\text{Me}_5$ ), 22.26, 27.41, 29.43 ( $\text{CHMe}_2$ ), 65.89, 96.14 (benzo), 114.39, 114.74, 120.42, 128.11 (Cp/benzo).

**Preparation of  $(\eta^5\text{-C}_9\text{H}_5\text{-1,3-(CHMe}_2)_2\text{)(}\eta^5\text{-C}_5\text{Me}_5\text{)ZrH}_2$  (**10-H}\_2\text{}**).** A J. Young NMR tube was charged with 0.040 g (0.094 mmol) of **10**, and benzene- $d_6$  was added. The tube was then frozen in liquid nitrogen degassed on a vacuum line, and an atmosphere of dihydrogen was admitted to the tube. Upon thawing, the tube was shaken for 2 min, during which time the solution turned from red to bright yellow. The tube was frozen again, and excess hydrogen was removed. Solvent removal in vacuo followed by recrystalli-

zation in pentane at  $-35\text{ }^{\circ}\text{C}$  yields 0.010 g (24%) of **10-H<sub>2</sub>** as a yellow solid. Anal. Calcd for  $\text{C}_{25}\text{H}_{36}\text{Zr}$ : C, 70.19; H, 8.48. Found: C, 70.02; H, 8.53.  $^1\text{H}$  NMR (benzene- $d_6$ ):  $\delta$  1.23 (d, 7 Hz, 6H,  $\text{CHMe}_2$ ), 1.35 (d, 7 Hz, 6H,  $\text{CHMe}_2$ ), 1.80 (s, 15H,  $\text{C}_5\text{Me}_5$ ), 3.36 (m, 2H,  $\text{CHMe}_2$ ), 6.78 (m, 2H, benzo), 7.14 (m, 2H, benzo), 7.27 (s, 2H, Zr-H), 7.88 (s, 1H, Cp).  $^{13}\text{C}$  NMR (benzene- $d_6$ ):  $\delta$  12.40 ( $\text{C}_5\text{Me}_5$ ), 22.05, 26.75, 27.87 ( $\text{CHMe}_2$ ), 110.59, 119.88, 121.20, 121.37, 122.75, 123.45 (Cp/benzo).

**Spectroscopic Identification of  $(\eta^5\text{-C}_9\text{H}_5\text{-1,3-(CHMe}_2)_2)(\eta^5\text{-C}_5\text{Me}_5)\text{ZrH}_2(\text{PMe}_3)$  (**10-H<sub>2</sub>(PMe<sub>3</sub>)**).** This compound was observed by a method similar to that used for **1-THI-H<sub>2</sub>(PMe<sub>3</sub>)**, using 0.010 g (0.023 mmol) of **10-H<sub>2</sub>** and 77 Torr (0.41 mmol) of  $\text{PMe}_3$  added via a calibrated gas bulb. Removal of excess  $\text{PMe}_3$  results in partial regeneration of **10-H<sub>2</sub>**.  $^1\text{H}$  NMR (toluene- $d_8$ ,  $23\text{ }^{\circ}\text{C}$ , 18 equiv of  $\text{PMe}_3$ ):  $\delta$  1.38 (d, 7 Hz, 6H,  $\text{CHMe}_2$ ), 1.58 (d, 7 Hz, 6H,  $\text{CHMe}_2$ ), 1.77 (br, 9H,  $\text{PMe}_3$ ), 1.81 (s, 15H,  $\text{C}_5\text{Me}_5$ ), 2.18 (s, 2H, Zr-H), 3.15 (m, 2H,  $\text{CHMe}_2$ ), 4.87 (s, 1H, Cp), 6.75 (m, 2H, benzo), 7.40 (m, 2H, benzo).  $^1\text{H}$  NMR (toluene- $d_8$ ,  $-70\text{ }^{\circ}\text{C}$ , 18 equiv of  $\text{PMe}_3$ ):  $\delta$  1.05 (br, 6H,  $\text{CHMe}_2$ ), 1.44 (br, 6H,  $\text{CHMe}_2$ ), 1.56 (br, 9H,  $\text{PMe}_3$ ), 1.85 (s, 15H,  $\text{C}_5\text{Me}_5$ ), 2.05 (d, 69 Hz, 2H, Zr-H), 3.27 (m, 2H,

$\text{CHMe}_2$ ), 4.84 (s, 1H, Cp), 6.82 (m, 2H, benzo), 7.35 (m, 2H, benzo).  $^{13}\text{C}$  NMR (toluene- $d_8$ ,  $-70\text{ }^{\circ}\text{C}$ , 18 equiv of  $\text{PMe}_3$ ):  $\delta$  13.07 ( $\text{C}_5\text{Me}_5$ ), 22.02 ( $\text{PMe}_3$ ), 25.52, 25.84, 29.96 ( $\text{CHMe}_2$ ), 111.23, 117.12, 118.14, 122.33, 124.02 (Cp/benzo). One Cp/benzo resonance was not located.  $^{31}\text{P}\{^1\text{H}\}$  NMR (toluene- $d_8$ ,  $-70\text{ }^{\circ}\text{C}$ , 18 equiv of  $\text{PMe}_3$ ):  $\delta$   $-16.67$ .

**Acknowledgment.** We thank the National Science Foundation (CAREER Award to P.J.C. and predoctoral fellowship to C.A.B.) for financial support. P.J.C. is a Cottrell Scholar supported by the Research Corp. and a David and Lucile Packard Fellow in Science and Engineering.

**Supporting Information Available:** Figures giving kinetic data and additional spectral data and a CIF file containing crystallographic data for **5-H<sub>2</sub>(PMe<sub>3</sub>)**. This material is available free of charge via the Internet at <http://pubs.acs.org>.

OM060035T